

# THE MAIN INJECTOR CHROMATICITY CORRECTION SEXTUPOLE MAGNETS: MEASUREMENTS AND OPERATING SCHEMES

C.M. Bhat, A.Bogacz, B.C. Brown, D.J. Harding, Si J. Fang, P.S. Martin, H.D. Glass and J.Sim  
 Fermi National Accelerator Laboratory\*  
 P.O. Box 500, Batavia, IL 60510

Abstract

The Fermilab Main Injector (FMI) is a high intensity proton synchrotron which will be used to accelerate protons and antiprotons from 8.9 GeV to 150 GeV. The natural chromaticities of the machine for the horizontal and the vertical planes are -33.6 and -33.9 respectively. The  $\Delta p/p$  of the beam at injection energy of 8.9 GeV is about 0.002. The chromaticity requirements of the FMI are primarily decided by the  $\Delta p/p = 0.002$  of the beam at injection. This limits the final chromaticity of the FMI to be  $\pm 5$  units. To correct the chromaticity in the FMI, two families of sextupole magnets will be installed in the lattice, one for each plane. A sextupole magnet suitable for the FMI needs has been designed [1] and are being built. New chromaticity compensation schemes have been worked out in the light of recently proposed faster acceleration ramps. On a R/D sextupole magnet, the low current measurements have been carried out to determine the electrical properties. Also with a Morgan coil, measurements have been performed to determine the higher ordered multipole components up to 18-poles. An overview of these results are presented here.

## I. CHROMATICITY COMPENSATION SCHEMES FOR THE FMI

Previously a scheme for chromaticity compensation in the FMI had been worked [2] out taking into account the effect of beam tube eddy current, saturation, and end-pack sextupole fields generated by the dipole magnets. The data were taken from measurements on R&D dipole magnets. Since then, several developments have taken place:

1. The measured [3] combined contribution of the saturation and static fields in the dipoles showed a slightly negative sextupole component (i.e.,  $b_2 = -0.05m^2$ ) at low fields (which is in contrast with the earlier scheme).
2. The material of the FMI beam tube is selected to be 316L stainless steel (resistivity of  $74 \times 10^8 Ohm m$ ) [4].
3. A faster ramp [4] is selected to reduce the emittance dilution at transition. The  $\dot{p}_t$  at transition in the present FMI operating scheme is about 280 GeV/c-sec, which is nearly a factor of two larger than the previously proposed ramp.

Hence, a new chromaticity compensation scheme has been developed. Here we essentially adopt the method outlined in the Ref. 2.

The Figs. 1 and 2 show examples of operating schemes for the FMI for two different values of  $\dot{p}$  at transition. The selection of  $\dot{p}_t = 280$  GeV/c-sec has resulted in a very large amount of

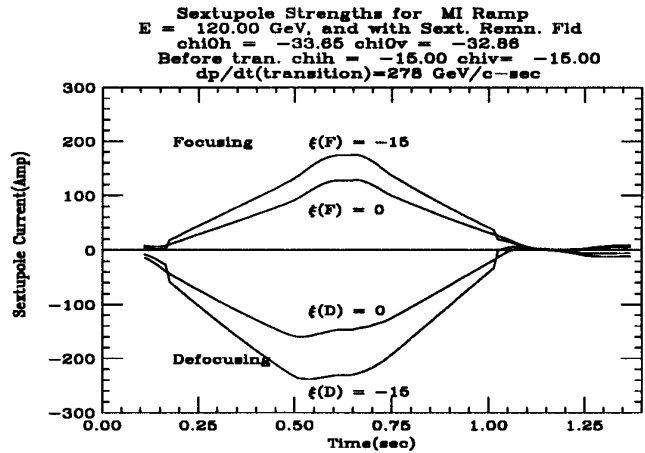


Figure 1. FMI Scheme for 120 GeV fast ramp

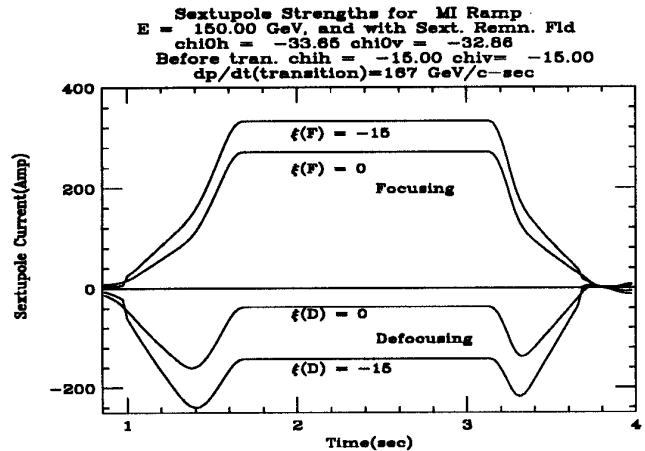


Figure 2. FMI scheme for 150 GeV slow ramp

eddy current contribution to the sextupole field at low B fields. For instance, the contribution to the sextupole component, that is arising from the eddy current reaches a maximum value of  $0.8 m^2$  for the ramps with  $\dot{p}_t = 280 GeV/c-sec$ . For the ramp with  $\dot{p}_t = 167/sec$ , the eddy current adds only about  $0.5m^2$  of sextupole strength. This suggested that with enough safety margin we might need a bipolar power supply for focusing family of sextupoles. For the de-focusing family however, the unipolar power supply should be sufficient.

## II. ELECTRICAL MODEL

The sextupole magnet is a three-terminal device with two coil terminals and one magnet case ground. The electrical characteristics of the magnet can be described by a 3x3 impedance matrix

\*Operated by the Universities Research Association, under contracts with the U.S. Department of Energy.

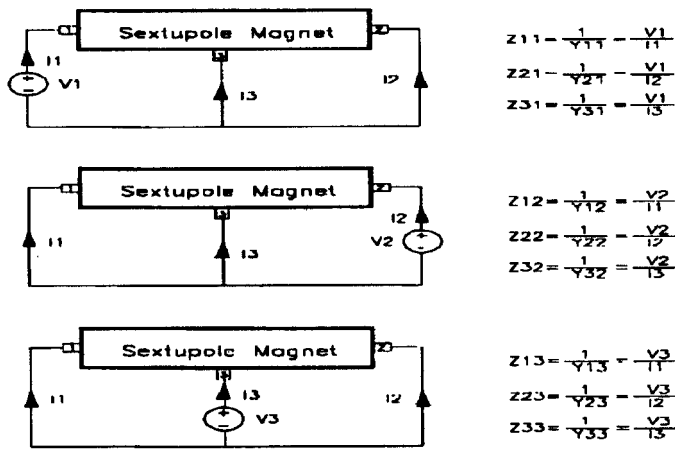


Figure 3. Impedance Matrix Measurement

at non-saturation. The equations for this three-terminal device network can be written as

$$\begin{bmatrix} I_1 \\ I_2 \\ I_3 \end{bmatrix} = \begin{bmatrix} Y_{11} & Y_{12} & Y_{13} \\ Y_{21} & Y_{22} & Y_{23} \\ Y_{31} & Y_{32} & Y_{33} \end{bmatrix} \begin{bmatrix} V_1 \\ V_2 \\ V_3 \end{bmatrix}$$

The elements in the matrix are frequency dependent variables. The magnet equivalent circuit can be determined by measuring the impedance matrix as shown in Fig. 3.

Terminal 1 and 2 are coil bus terminals and terminal 3 is the case ground.  $Z_{11}$ ,  $Z_{22}$ ,  $Z_{12}$  and  $Z_{22}$  measure the coil bus impedance. Total bus to ground capacitance is measured by  $Z_{33}$ ,  $Z_{13}$  and  $Z_{31}$  measure the capacitance between terminal 1 and ground, while terminal 2 is shorted to ground. Similarly,  $Z_{23}$  and  $Z_{32}$  measure the capacitance between terminal 2 and ground, while terminal 1 is grounded. The  $Z_{13}$ ,  $Z_{23}$  and  $Z_{33}$  are capacitance measurements since the slope of the measurements data is -20 dB/decade in Bode plot.

The circuit simulation program Spice is used to curve fitted the sextupole magnet electrical model into its impedance matrix as shown in Fig.4 for  $Z_{11}$ .

Figure 5 shows the sextupole magnet electrical model. T1 represents the copper loss and R2 is for the core loss. L1 and R3 are the air core inductance and skin depth effects respectively

### III. MAGNET MEASUREMENTS

The magnets are measured at the Fermilab Magnet Test facility (MTF) using a rotating Morgan coil with the database-controlled MTF software [5]. The coil is rotated at the center of the magnet at a constant current. Activating different coil windings allows the measurements of the sextupole strength and the contributions to the field shape from other harmonic components up to 18 poles. In these measurements we have measured both normal as well as skew components. We find none of the components are of significant importance for FMI operation scheme except the remnant field. A remnant field of  $-0.3(\text{Tm}/\text{m}^2)$  seen for the magnet that is ramped up to 350 Amp. Using the scheme outlined in Ref.6 we have extracted the non-linear part of the sextupole field. The result is shown in Fig. 6. In our chromaticity compensation scheme developed for FMI in section I,

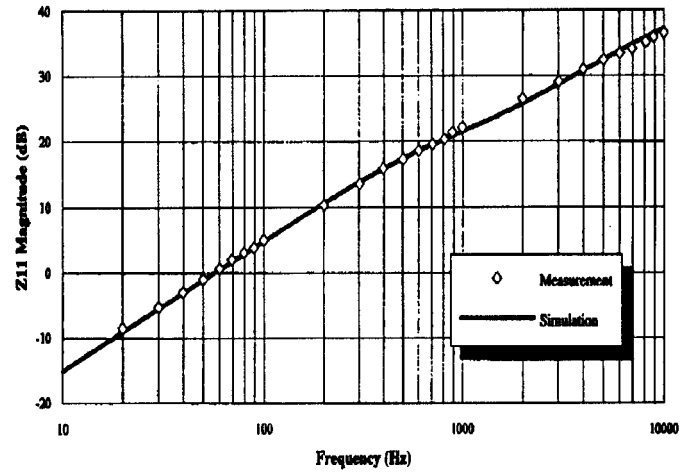


Figure 4.  $Z_{11}$  Magnitude Plot

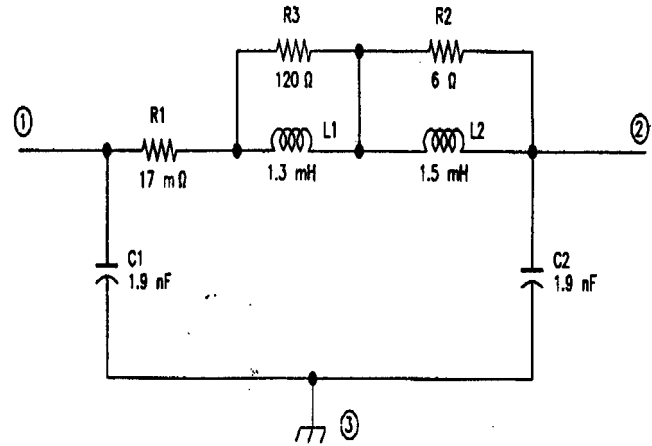


Figure 5. Main Injector Sextupole Electrical Model

we have included this non-linear part of the sextupole field. The sextupole field arising from the eddy current and the remnant field of the sextupole magnet counteract. Hence, the focusing sextupole magnet power supplies need not go much negative.

Authors would like to thank the MTF personnel for their help during the magnet measurements.

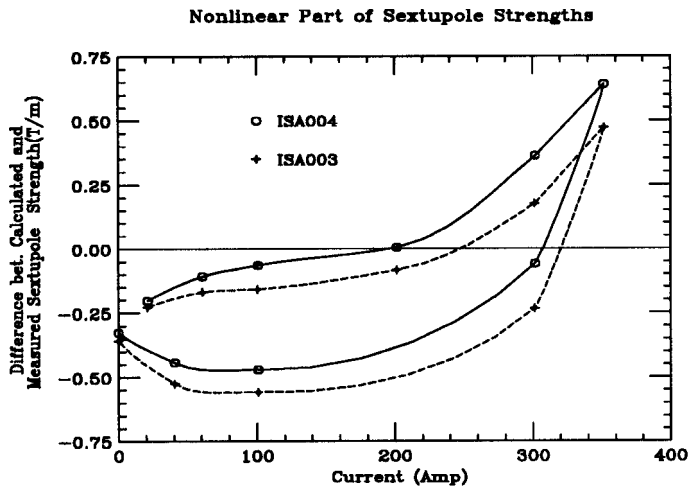


Figure 6. Impedance Matrix Measurement

### References

- [1] D.J. Harding, N.Chester, and R. Baiod, Proc. of Part. Accel. Conf. (1993) 2826.
- [2] S.A. Bogacz, Proc. of Part. Accel. Conf. (1993) 77.
- [3] H. D. Glass, Private Communication.
- [4] The Main Injector Technical Design Handbook 1994.
- [5] J.W. Sim *et al.*, "Software for a Database-Controlled Measurements System at Fermilab Magnet Test Facility" (these proceedings).
- [6] B.C. Brown, "Analysis of Magnet Strengths from Steel B-H Curves and Geometry", Fermilab MTF-94-0078, (1994).